Hidemasa Uematsu, MD
Masayuki Maeda, MD
Norihiro Sadato, MD
Tsuyoshi Matsuda, RT
Yoshiyuki Ishimori, RT
Yoshio Koshimoto, MD
Hiroki Yamada, MD
Hirohiko Kimura, MD
Yasutaka Kawamura, MD
Tetsuya Matsuda, MD
Nobushige Hayashi, MD
Yoshiharu Yonekura, MD
Yasushi Ishii, MD

Index terms:
Brain, MR, 13.121411, 13.121412
Brain, neoplasms, 13.3641, 13.366
Magnetic resonance (MR), diffusion study, 13.12144
Magnetic resonance (MR), perfusion study, 13.12144
Magnetic resonance (MR), tissue characterization, 13.121411, 13.121412
Meninges, MR, 139.121411, 139.121412
Meninges, neoplasms, 139.366

Radiology 2000; 214:912–917

Abbreviations:
$\Delta R2^*$ = T2* rate change
$\Delta R2^*_{TIC}$ = T1-corrected change in R2* from the double-echo data
$\Delta R2^*_{TICf}$ = gamma-fitted $\Delta R2^*_{TIC}$ data
$\Delta R2^*_{TIU}$ = T1-uncorrected change in R2* from the single-echo data

[1] From the Department of Radiology (H.U., M.M., Y. Ishimori, Y. Koshimoto, H.Y., H.K., Y. Kawamura, N.H., Y. Ishii) and the Biomedical Imaging Research Center (N.S., Y.Y.), Fukui Medical University, 23 Shimoaizuki, Matsuoka-cho, Yoshida-gun, Fukui, 910-1193 Japan; GE-Yokogawa Medical Systems, Tokyo, Japan (Tsuyoshi M.); the Department of Medical Informatics, Kyoto University Hospital, Kyoto, Japan (Tetsuya M.); and the Department of Cerebral Research, National Institute for Physiological Sciences, Okazaki, Japan (N.S.). Received July 31, 1998; revision requested September 11; final revision received June 28, 1999; accepted August 12. Supported in part by research grant JSPS-RFTF97L00203 from the Japan Society for the Promotion of Science and by an international exchange grant from the Japan Society of Magnetic Resonance in Medicine. **Address reprint requests to H.U.** (e-mail: *uematsu@fmsrsa.fukui-med.ac.jp*).

Author contributions:
Guarantors of integrity of entire study, H.U., M.M., N.S.; study concepts and design, H.U.; definition of intellectual content, H.U., M.M., N.S.; literature research, H.U., M.M., N.S.; clinical studies, H.U., M.M., H.Y., H.K., Y. Koshimoto, Y. Kawamura; data acquisition, Tsuyoshi M., Y. Ishimori; statistical analysis, H.U.; manuscript preparation, H.U.; manuscript editing, M.M., N.S.; manuscript review, Tetsuya M., N.H., Y.Y., Y. Ishii.

Vascular Permeability: Quantitative Measurement with Double-Echo Dynamic MR Imaging—Theory and Clinical Application[1]

Double-echo dynamic magnetic resonance (MR) imaging was used to evaluate both vascularity and permeability of tissues simultaneously. Vascularity was evaluated on the basis of the T2*-shortening effect due to the intravascular fraction of the contrast agent and permeability on the basis of the T1-shortening effect due to the extravascular fraction. Meningioma was characterized on the basis of higher vascularity and neurinoma on the basis of higher permeability. The proposed method enables better tissue characterization.

The contrast material–enhanced magnetic resonance (MR) imaging technique is widely used for detection and characterization of lesions (1–4). Contrast agents such as gadopentetate dimeglumine (Magnevist; Nihon Schering, Osaka, Japan) cause T1 shortening once they leak into the interstitial space. The amount of leaked contrast agent can be determined on the basis of its extraction fraction (or permeability of the vessels) multiplied by perfusion; therefore, contrast-enhanced MR imaging reflects both permeability and perfusion of the tissue. On the other hand, contrast agents that remain in the vascular space cause a signal intensity decrease as a result of the increased inhomogeneity of local magnetic fields (T2* shortening effect [5–9]). This characteristic is used to evaluate semiquantitatively the cerebral perfusion (5–9) or tumor vascularity (10–15).

The purposes of the present study were to propose a method for evaluating both vascularity and permeability of tissues simultaneously, with use of gadolinium-enhanced and dynamic MR imaging acquisitions with a double-echo technique (14), and to realize a better differentiation between meningioma and neurinoma, both of which show intense contrast enhancement (1).

Materials and Methods

Theory

After bolus injection, gadopentetate dimeglumine causes a T2* rate change ($\Delta R2^*$) in permeable tissue that is contaminated by T1-shortening effect due to a leakage of the contrast material (12,13). The T1-shortening effect can be corrected by using double-echo technique (14). As this effect is near linearly related to the concentration of the leaked contrast material, it can be used as an index for contrast material leakage:

$$LV = \Delta R2^*_{TIC}(t) - \Delta R2^*_{TIU}(t) \; (t > t_0), \quad (1)$$

where LV is the leakage value, t is time, $\Delta R2^*_{TIU}$ is the T1-uncorrected $\Delta R2^*$ from the single-echo data, and $\Delta R2^*_{TIC}$ is the T1-corrected $\Delta R2^*$ from the double-echo data. Note that the leakage value should be constant after the first pass ends ($t > t_0$), and the leakage value reflects the total amount of the leaked contrast agent, not the permeability or extraction fraction itself. On the other hand, the vascularity value (relative blood volume) (VV) can be estimated on the basis of the T2*-shortening effect of the intravascular contrast material by using the following equation, fitted with gamma function ($\Delta R2^*_{TICf}$) to eliminate the second-pass effect (16):

$$VV = \int_0^\infty \Delta R2^*_{TICf}(\tau)\, d\tau, \quad (2)$$

where τ is time.

The leakage value can be normalized by the maximum height of the curve of $\Delta R2^*_{T1Cf}$ to derive the leakage index (LI):

$$LI = \frac{\Delta R2^*_{T1C}(t) - \Delta R2^*_{T1U}(t)}{\Delta R2^*_{T1Cf}\ max}. \quad (3)$$

The vascularity value of the tumor can be normalized by that of the reference tissue (white matter, for example) to generate the vascularity index. A detailed description is seen in the Appendix.

Subjects

Human studies were performed under the guidelines of the committee on clinical investigations at Fukui Medical University. Written informed consent was obtained from all patients. Eleven consecutive patients (three men and eight women; age range, 26–76 years; mean age, 49.5 years) with acoustic neurinomas and eleven consecutive patients (two men and nine women; age range, 38–73 years; mean age, 56.5 years) with meningiomas were included in the study population. The histologic subtype of the meningiomas was meningotheliomatous in seven patients, transitional in two, fibrous in one, and clear cell in one. All neurinomas originated in the acoustic nerve, and in each case the histologic diagnosis was available. The maximum diameters of meningiomas and neurinomas ranged from 2.0 to 6.0 cm (mean, 3.32 cm) and from 1.5 to 4.0 cm (mean, 2.28 cm), respectively. The diameter of the neurinomas in the vicinity of the internal auditory canal was 1.5 cm or larger; therefore, detection was not hindered by susceptibility artifacts from the mastoid bone.

MR Imaging Techniques

Transverse T1-weighted spin-echo images (repetition time msec/echo time msec = 333/10 with three signals acquired) and T2-weighted fast spin-echo images (3,500/88 [effective] with two signals acquired) were obtained (rectangular field of view, 22 × 16 cm; matrix, 256 × 224; section thickness, 5 mm) with use of a 1.5-T MR system (Horizon; GE Medical Systems, Milwaukee, Wis) before the dynamic study.

For dynamic studies of all patients, we used two echoes with echo times of 7 and 23 msec spoiled gradient-recalled acquisition in the steady state, or SPGR, sequence (33.3/7, 23; flip angle, 10°; 0.75 signal acquired; matrix, 256 × 128; section thickness, 7 mm; rectangular field of view, 24 × 16 cm). The dynamic images were obtained at the level of a single section that corresponded to the levels of the most appropriate abnormalities seen on nonenhanced MR images obtained in selected patients with brain tumors. After five images were acquired, gadopentetate dimeglumine (0.15 mmol per kilogram of body weight) was rapidly injected intravenously at a rate of 4 mL/sec with an MR-compatible power injector (MRS-50; Nemoto, Tokyo, Japan), followed by a 20-mL saline solution flush. After administration of the bolus of gadopentetate dimeglumine, a dynamic series of 50 sets of double-echo images were obtained at 2.4-second intervals. For this sequence, the total acquisition time was approximately 2 minutes. After the dynamic studies, we also obtained contrast-enhanced T1-weighted spin-echo images.

Data Analysis

Region-of-interest analysis.—Regions of interest were placed by one radiologist (H.U.) in both the normal white matter and the solid portion of tumors. Time series of signal intensity were converted to changes in $\Delta R2^*_{T1C}$ and $\Delta R2^*_{T1U}$ (Appendix). Gamma fitting (16) of $\Delta R2^*_{T1C}$ data was performed to generate $\Delta R2^*_{T1Cf}$. The vascularity values were then obtained by means of Equation (2), and the vascularity index of the tumor was calculated with the vascularity value of the tumor normalized by that of the white matter. To obtain the leakage value, five points of $(\Delta R2^*_{T1C} - \Delta R2^*_{T1U})$ values immediately after the first pass of time-to-$\Delta R2^*_{T1Cf}$ curve were averaged.

Parametric maps.—Parametric images of the vascularity and leakage indexes were generated for each subject by using in-house software. MR images were transferred to a workstation (Ultra1 Creator 3D; Sun Microsystems, Mountain View, Calif). On a pixel-by-pixel basis, the signal intensity was converted to changes in $\Delta R2^*_{T1C}$ and $\Delta R2^*_{T1U}$. To obtain the vascularity value, we used a simple numeric integration of time-to-$\Delta R2^*_{T1C}$ curve across a user-specified time interval instead of gamma fitting, because gamma fitting on a pixel-by-pixel basis is difficult due to the relatively low signal-to-noise ratio on the dynamic images. The leakage value was obtained by using the same procedure as in the region-of-interest analysis, on a pixel-by-pixel basis.

Statistical Analysis

For both meningiomas and neurinomas, a statistical review of the vascularity and leakage indexes was performed with the Mann-Whitney *U* test. A *P* value of less than .05 was considered statistically significant.

Results

As shown in Figure 1, a typical meningioma was characterized by a high $\Delta R2^*_{T1Cf}$ curve and low leakage values relative to the gamma-fitted $\Delta R2^*$ curve of the normal white matter (Fig 1a), which resulted in a high vascularity index and a relatively low leakage index (Fig 1b). Note that the time-to-leakage value was constant after the first pass ended. Conversely, a typical neurinoma was characterized by a large leakage value, and the height of the $\Delta R2^*_{T1Cf}$ curve was similar to the height of the gamma-fitted $\Delta R2^*$ of the white matter (Fig 2a). This resulted in a vascularity index similar to that of the normal white matter and a leakage index higher than that of meningioma (Fig 2b). These characteristics are summarized in Figure 3.

The mean vascularity index of the meningiomas was significantly higher than that of the neurinomas (mean, 9.88 ± 9.99 [SD] [meningiomas] vs 2.14 ± 1.71 [neurinomas], $P = .0043$, Mann-Whitney *U* test), although in some cases the vascularity index overlapped between the two types of tumors. Three patients with meningiomas (meningotheliomatous, $n = 2$; clear cell, $n = 1$) showed high vascularity index values.

The leakage values for all patients in the study ranged from 3.15 to 11.40 (mean, 6.99 ± 2.12). The mean leakage index of the neurinomas was significantly higher than that of the meningiomas (mean, 0.27 ± 0.08 [meningiomas] vs 0.88 ± 0.32 [neurinomas], $P = .001$, Mann-Whitney *U* test). The leakage index separated the two types of neoplasms except in one case.

Discussion

Findings in the present study showed that permeability and vascularity of tumors can be evaluated separately by using a rapid dynamic sequence that requires only 2 minutes. These two parameters successfully characterized the neurinoma and meningioma, with the leakage index particularly useful in the differentiation.

Findings in the simulation study (Appendix) showed a nearly linear relationship between the leakage value and T1 change ($\Delta R1$) with long $T1_0$ (>1.0 second) and within a certain range of leakage values (from 0 to 12). Note that $T1_0$ and T1 are the T1 values before and after

the arrival of the contrast agent, respectively. When $T1_0$ of tumors, as measured with a 1.5-T system, is greater than 1.0 (17), the leakage value in most cases observed in this study was less than 12, with the leakage value reflecting the concentration of the contrast agent in the extravascular space. The time-to-leakage value remained constant after the first pass ended, which confirmed our assumption that there is no back diffusion of the contrast agent, at least in the case of meningiomas and neurinomas.

Vascularity has been used to characterize the neoplastic process. Maeda et al (10) suggested that vascularity evaluated on the basis of the time-to-$\Delta R2^*_{T1U}$ curve was significantly higher in meningiomas than in neurinomas, even with contamination of the T1-shortening effect caused by the contrast agent leaking into the extravascular space. Findings in the present study confirmed that meningiomas were characterized by higher vascularity than were neurinomas, although there was substantial overlap even with correction for the T1-shortening effect.

In characterization of the neoplastic process, it is essential to include leakage of the contrast agent into the extravascular space, but, to our knowledge, few studies have been performed to attempt to quantify it (18,19). In these studies, pharmacokinetic two-compartment models are used to quantify the leakage of gadopentetate dimeglumine, assuming a linear relationship between the change in R1 and the tissue concentration of gadopentetate dimeglumine and a multiexponential decay of plasma concentration of gadopentetate dimeglumine. Low temporal resolution of tissue T1 measurements, arterial blood sampling, and complicated curve analysis are cumbersome in a clinical setting. In the present study, we quantified the amount of the leaked contrast material during the first pass by measuring its counter effect on the T2* shortening due to the intravascular fraction of the contrast agent (the leakage value). Note that the leakage value reflects the total amount of the leaked contrast material and not the permeability or extraction fraction itself. Hence, we normalized the leakage value with the maximum height of $\Delta R2^*_{T1Cf}$ to obtain the leakage index. As $\Delta R2^*_{T1Cf}$max is known to be proportional to blood flow, the leakage index may in part reflect tissue permeability.

In the present study, we attempted to differentiate meningiomas and neurinomas, because they frequently originate in similar locations such as the cerebellopontine angle and the skull base, with similar patterns of contrast enhancement. Differential diagnosis is usually possible when morphologic characteristics are found such as extension along the course of cranial nerves in neurinomas or dural enhancement adjacent to the tumor in meningiomas (20,21). Previous attempts at tissue characterization on the basis of signal intensity differences or relaxation time measurements resulted in considerable overlap (21,22).

Our data showed that the leakage indexes of neurinomas were much larger than those of meningiomas except in one case, which suggests that neurinomas are more permeable to contrast media in tumor vessels than are meningiomas. This is consistent with findings in the study by Watabe and Azuma (23), who reported that an injection of gadopentetate dimeglumine caused a greater T1 increment in neurinomas than in meningiomas. This indicates that the contrast material achieved greater access into extravascular spaces in neurinomas.

According to findings in previous studies (23,24), endothelial fenestration and

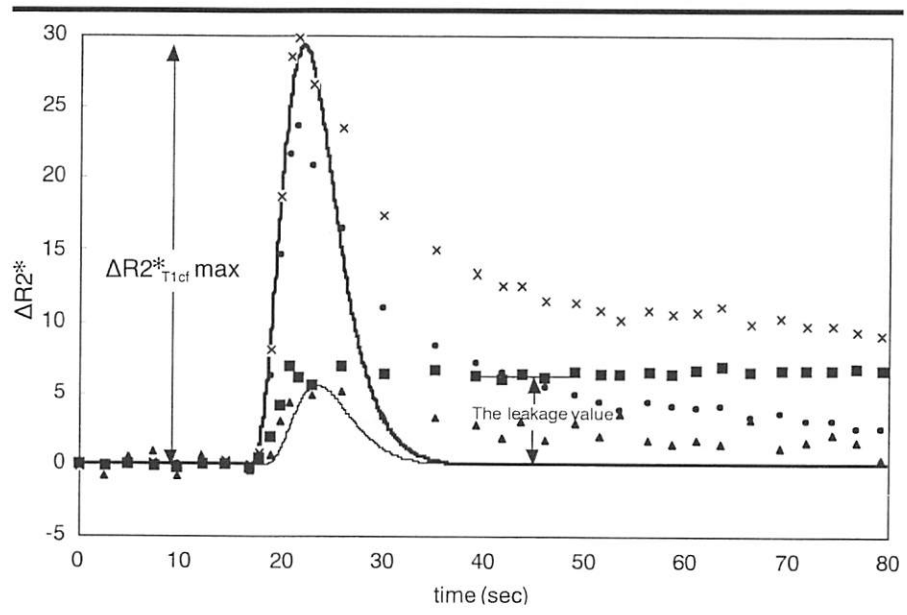

a.

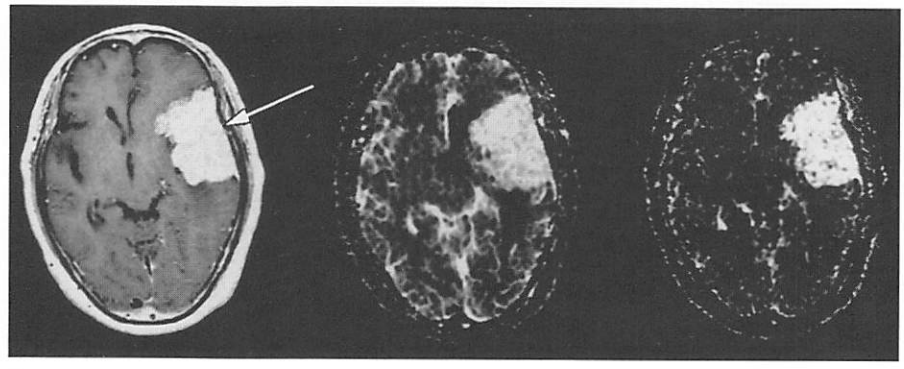

b.

Figure 1. Meningioma. **(a)** Time course of the ΔR2* values of the meningioma and the normal white matter in a 57-year-old woman. $\Delta R2^*_{T1C}$ values of the meningioma = *X*, $\Delta R2^*_{T1Cf}$ = bold line, $\Delta R2^*_{T1U}$ = ●. $\Delta R2^*_{T1C} - \Delta R2^*_{T1U}$ (■) is constant after the first pass ends, and the leakage value is relatively small compared with the height of $\Delta R2^*_{T1Cf}$ ($\Delta R2^*_{T1Cf}$max). The $\Delta R2^*_{T1C}$ values of the normal white matter (▲) with their gamma-fitted curve (fine line) show that the height of $\Delta R2^*_{T1C}$ of meningiomas was higher than that of normal white matter. The vascularity value of meningiomas was much larger (516.77) than that of normal white matter (75.26). **(b)** Contrast-enhanced T1-weighted spin-echo MR image (left), the vascularity index map (middle), and the leakage index map (right) in the same patient. Meningioma shows intense contrast enhancement on the image on the left (white arrow). Note the high vascularity index of the meningioma in the left front temporal region.

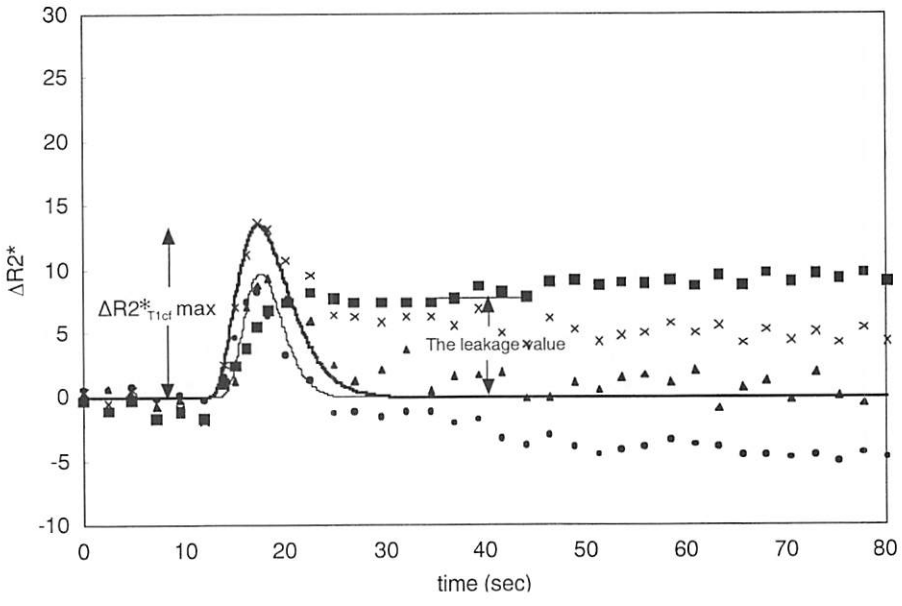

a.

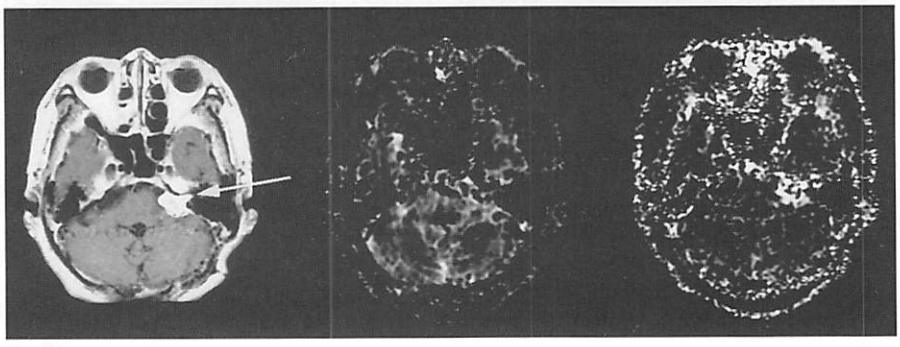

b.

Figure 2. Neurinoma. **(a)** Time course of the ΔR2* values of the neurinoma and the normal white matter in a 67-year-old woman. $\Delta R2^*_{T1C}$ values of the neurinoma = X with their gamma-fitted curve (bold line), $\Delta R2^*_{T1U}$ = ●, $\Delta R2^*_{T1C} - \Delta R2^*_{T1U}$ = ■, $\Delta R2^*_{T1C}$ values of the normal white matter = ▲ with their gamma-fitted curve (fine line). The vascularity value of the neurinoma was slightly larger (213.43) than that of normal white matter (111.6). The average leakage value of the neurinoma was relatively large (7.54) compared with the $\Delta R2^*_{T1Cf}$max (13.47), which caused a larger leakage index (0.56). **(b)** Contrast-enhanced T1-weighted spin-echo image (left), vascularity index map (middle), and leakage index map (right) of the neurinoma in the left cerebellopontine angle. Neurinoma shows intense contrast enhancement on the left image (white arrow). Note the relatively low vascularity index and high leakage index of the tumor.

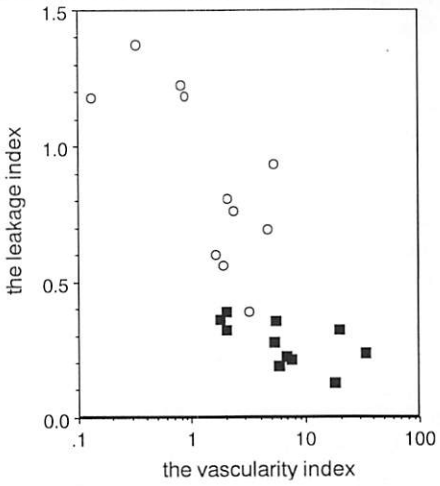

Figure 3. Semilogarithmic plot of the leakage index and vascularity index of meningiomas (■, n = 11) and neurinomas (○, n = 11). There is a substantial overlap of the vascularity index between the two types of tumors. The leakage index separated them except in one case.

open-gap junctions, which are commonly found in the capillaries of neurinomas and meningiomas, function as routes into the extravascular space, where the T1 effect of gadopentetate dimeglumine can be achieved. The capillary structures in neurinomas are simple, and the gap junctions are usually short, straight, and patent (24), freely communicating with extravascular space. In meningiomas, on the other hand, the gap junctions are often tortuous, elongated, and sinusoidal, and they are frequently lined with abnormal endothelial cells similar to tumor cells (24). The difference in gap junctions between the two types of tumors may explain why, during the first transit, the contrast agent achieves greater and faster access into the extravascular space in neurinomas, which causes a larger leakage index in neurinomas than in meningiomas.

Although the proposed indexes provide acceptable results for differentiating neurinomas and meningiomas, further studies with more patients are necessary to confirm the usefulness of our theory.

In conclusion, dynamic contrast-enhanced MR imaging with double-echo technique can allow separate evaluation of both the permeability and vascularity of tumors. A differential diagnosis of meningioma and neurinoma may be possible with use of this technique.

Appendix

After bolus injection, a contrast agent such as gadopentetate dimeglumine is extracted from intravascular into extravascular space. With a simple two-compartment model, assuming no back diffusion and no recirculation effect, the extraction fraction (E) of the contrast agent is

$$E = \frac{C_T}{F \cdot \int_0^\infty C_A(\tau)\, d\tau}, \qquad \text{(A1)}$$

where C_T represents the concentration of the contrast agent in the extravascular space of the tissue, which is constant after the first pass ends ($\tau > t_0$), F represents the regional blood flow, and $C_A(\tau)$ represents the input function. The relationship between the concentration of the contrast agent in the tissue vessels at the time $\tau[C_V(\tau)]$ and $C_A(\tau)$ is given with the following:

$$C_T + F \cdot \int_0^\infty C_V(\tau)\, d\tau = F \cdot \int_0^\infty C_A(\tau)\, d\tau, \qquad \text{(A2)}$$

where we assume that the arterial component of the tissue is negligible compared with the nonarterial tumor vessels. The ratio of the blood volume to regional blood flow V/F, or the mean transit time

(MTT), is given with the following (25) equation:

$$V/F = \mathrm{MTT} = \frac{\int_0^\infty C_V(\tau)\, d\tau}{C_V \max}, \quad \text{(A3)}$$

where $C_V$max represents the maximum height of the curve $C_V(\tau)$. Hence, E is given with

$$E = \frac{C_T}{C_V \max \cdot V + C_T} = \frac{C_T/C_V \max}{V + C_T/C_V \max}. \quad \text{(A4)}$$

As MR imaging cannot directly quantify the concentration of the contrast agent in the intravascular or extravascular space or absolute blood volume, neither E nor permeability can be calculated directly. However, Equation (A4) gives a clue about how to generate useful indexes for characterization of neoplastic tissues.

Bolus injection of a paramagnetic contrast agent such as gadopentetate dimeglumine causes MR signal changes due to a change in relaxation times (T1, T2, T2*). The relationship between the MR signal (S) of a gradient echo and the relaxation time can be expressed as follows (26):

$$S \propto \rho \frac{[1 - \exp(-TR/T1)] \times \exp(-TE/T2^*) \cdot \sin\alpha}{1 - \exp(-TR/T1) \cdot \cos\alpha}, \quad \text{(A5)}$$

where ρ is the proton density, α is the flip angle, TR is the repetition time, TE is the echo time, and T1 is the tissue T1 value. When images are obtained before and after the injection of a contrast agent, one can combine these equations and then eliminate ρ and sin α, so that the equations become

$$\Delta R2^* = -\ln(S/S_0)/TE + \ln\left[\frac{1 - \exp(-TR/T1)}{1 - \exp(-TR/T1_0)}\right]\Big/TE + \ln\left[\frac{1 - \exp(-TR/T1_0) \cdot \cos\alpha}{1 - \exp(-TR/T1) \cdot \cos\alpha}\right] \div TE, \quad \text{(A6)}$$

where $\Delta R2^*$ is the T2* rate change [$\Delta(1/T2^*)$]; S_0 and S are the MR signals before and after the arrival of the contrast agent, respectively; and $T1_0$ and T1 are the T1 values before and after the arrival of the contrast agent, respectively.

If the contrast agent remains in the vascular space without leaking into the interstitial space, as would be the case in a normal brain with an intact blood-brain barrier, the T1 of the tissue is not affected by the contrast agent: $T1 \simeq T1_0$. Hence, Equation (A6) can be simplified as follows (5–13):

$$\Delta R2^* = -\ln(S/S_0)/TE. \quad \text{(A7)}$$

The area under the time-to-$\Delta R2^*$ curve is proportional to the relative regional cerebral blood volume (rrCBV), on the basis of the linear relationship between $\Delta R2^*$ and the local concentration of the paramagnetic contrast agent and the principles of the indicator dilution theory for nondiffusible intravascular tracers (5):

$$\mathrm{rrCBV} \propto \int_0^\infty \Delta R2^*\, dt. \quad \text{(A8)}$$

Contributions of tracer recirculation must be eliminated before volume information can be extracted. The fitted gamma variate curve has been used to eliminate second-pass effects (16):

$$\Delta R2^* = K(t - t_0)^\alpha e^{-(t-t_0)/\beta}, \quad \text{(A9)}$$

where K represents the constant scale factor, t represents time after injection, and t_0 represents the arrival time of the contrast material bolus. The α and β represent arbitrary parameters determined by means of nonlinear least squares fit. The fitted gamma variate curve is used to extrapolate the concentration curve and approximate its appearance while avoiding the confounding recirculation effects of the contrast agent.

Even during the first pass, gadopentetate dimeglumine enters the extravascular space of many tissues, except for the central nervous system with an intact blood-brain barrier. Leakage of gadopentetate dimeglumine has two effects on changes in the signal intensity of tissues. First, the loss of field heterogeneity between the vessels and the surrounding tissues affects $[-\ln(S/S_0)/TE]$ in Equation (A6)(10); this effect was not considered in this study. Second, when leaked, gadopentetate dimeglumine shortens the T1 of the tissues,

$$\ln\left[\frac{1 - \exp(-TR/T1)}{1 - \exp(-TR/T1_0)}\right]\Big/TE + \ln\left[\frac{1 - \exp(-TR/T1_0) \cdot \cos\alpha}{1 - \exp(-TR/T1) \cdot \cos\alpha}\right]\Big/TE$$

in Equation (A6) increases. Therefore, if we apply Equation (A7) to permeable tissue, the value of $\Delta R2^*$ will be underestimated due to a leakage of the contrast agent ($\Delta R2^*_{T1U}$ = $\Delta R2^*$ uncorrected for T1 shortening) (12,13).

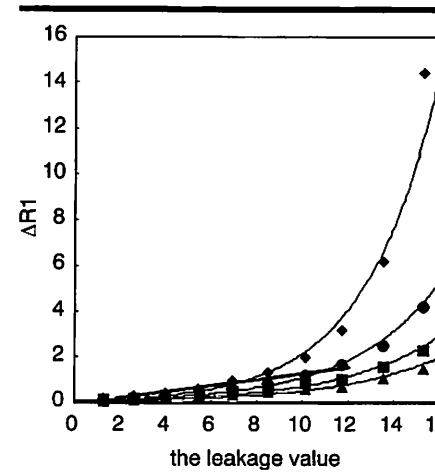

Figure 4. Scatterplot of simulated $\Delta R1$ values versus the leakage value. $T1_0$ values = 1.0 (◆), 1.2 (●), 1.4 (■), and 1.6 (▲) seconds. In the range of the leakage value less than 12, where all the observed values in the present study are included, $\Delta R1$ values and the leakage value with $T1_0$ of 1.2 second demonstrates a nearly linear relationship (r^2 = 0.94, straight bold line). In the range of the leakage value less than 16, the relationship is actually exponential (r^2 = 0.98, 0.97, 0.96, 0.96 for $T1_0$ = 1.0, 1.2, 1.4 and 1.6 seconds, respectively).

Miyati et al (14) evaluated tumor vascularity with correction for T1 shortening by using double-echo MR imaging. R2* is

$$R2^* = \ln[S(TE1)/S(TE2)]/(TE2 - TE1), \quad \text{(A10)}$$

where R2* is the T2* rate (1/T2*), and $S(TE_1)$ and $S(TE_2)$ represent the signal of the first TE and the second TE, respectively. Consequently, $\Delta R2^*$ with correction to T1 shortening ($\Delta R2^*_{T1C}$) is

$$\Delta R2^*_{T1C} = R2^* - R2^*_0, \quad \text{(A11)}$$

where $R2^*_0$ is the T2* rate before the arrival of the contrast agent. Hence, in a permeable tissue, the vascularity value that represents tissue vascularity (relative blood volume) is given with the following equation with $\Delta R2^*$ corrected for T1 shortening ($\Delta R2^*_{T1C}$) (14) fitted with the gamma function to eliminate the second-pass effect (16):

$$VV = \int_0^\infty \Delta R2^*_{T1Cf}\, dt. \quad \text{(A12)}$$

As the vascularity value VV is a relative regional blood volume, it can be normalized by means of comparison with the

vascularity value of the reference tissue (white matter, for example) to generate the vascularity index.

Miyati et al (14) did not point out that the correction factor for the T1-shortening effect may be used as an index for contrast material leakage. Denote as $\Delta R2^*_{T1U}$ the T1-uncorrected $\Delta R2^*$ that was calculated from the single-echo MR data (from Eq [A7]). If the concentration of the contrast agent in the extravascular space of the tissue (C_T) and $\Delta R2^*_{T1C}(t) - \Delta R2^*_{T1U}(t)(t > t_0)$ are related linearly, the latter can be used as a parameter of contrast material leakage to extravascular space. An index of the leaked contrast agent (the leakage value LV) is given with the following:

$$LV = \Delta R2^*_{T1_C}(t) - \Delta R2^*_{T1U}(t)$$

$$\approx \ln\left[\frac{1 - \exp(-TR/T1)}{1 - \exp(-TR/T1_0)}\right]\Big/TE$$

$$+ \ln\left[\frac{1 - \exp(-TR/T1_0)\cdot\cos\alpha}{1 - \exp(-TR/T1)\cdot\cos\alpha}\right]\Big/TE$$

($t > t_0$; after first pass ended). (A13)

Note that the leakage value should be constant after the first pass ends, and the leakage value reflects the total amount of the leaked contrast agent, not the permeability or extraction fraction itself. Hence, the leakage index LI is derived from the leakage value normalized with $\Delta R2^*_{T1C}$max:

$$LI = \frac{\Delta R2^*_{T1C}(t) - \Delta R2^*_{T1U}(t)}{\Delta R2^*_{T1C}\ max}, \quad (A14)$$

where $\Delta R2^*_{T1C}$max represents the maximum height of the curve $\Delta R2^*_{T1C}$. As $\Delta R2^*_{T1C}$max is known to be proportional to blood flow (25), the leakage index may in part reflect tissue permeability.

Simulation of the relationship between the leakage value and the concentration of the contrast agent.—We performed a computer simulation to evaluate the relationship between the leakage value and the concentration of the contrast agent. The simulation was based on the fact that both the leakage value and concentration of the contrast agent in the extravascular space are related to T1 values with and those without contrast material. The leakage value is given with Equation (A13), with the flip angle (α = 10°), repetition time (TR = 33.3 msec), and second echo time (TE = 23 msec) fixed to match those used in our study.

Denote $\Delta R1$ as $(1/T1 - 1/T1_0)$. Since the linear relationship between $\Delta R1$ and the tissue concentration of the contrast agent is well known (5), $\Delta R1$ was plotted against the leakage value by changing T1. T1 is expressed with $T1_0$ as

$$T1 = T1_0 - \Delta T1,$$

where $\Delta T1$ is the shortened T1 due to the leaked contrast material. Assuming $T1_0$ of 1.2 second, the most representative T1 value of neoplasms measured with a 1.5-T system (17), the leakage value was plotted against $\Delta R1$ by changing $\Delta T1$ from 0.1 to 1.2 seconds with a step of 0.1 second. We performed similar simulations with $T1_0$ of 1.0, 1.4, and 1.6 seconds.

Results of the simulation.—Figure 4 shows the simulated plot of $\Delta R1$ against the leakage value. With $T1_0$ of 1.2 second, in the range of leakage values from 0 to 12, a nearly linear relationship was found (r^2 = 0.94), whereas an exponential relationship was demonstrated with a wider range from 0 to 16. The relationship became more linear as $T1_0$ grew larger.

Acknowledgment: The authors thank Hiroyuki Sashie, RT, for assistance with MR imaging data collection.

References

1. Fujii K, Fujita N, Hirabuki N, Hashimoto T, Miura T, Kozuka T. Neuromas and meningiomas: evaluation of early enhancement with dynamic MR imaging. AJNR Am J Neuroradiol 1992; 13:1215–1220.
2. Edelman RR, Li W. Contrast-enhanced echo-planar MR imaging of myocardial perfusion: preliminary study in humans. Radiology 1994; 190:771–777.
3. Hatabu H, Gaa J, Kim D, Li W, Prasad PV, Edelman RR. Pulmonary perfusion: qualitative assessment with dynamic contrast-enhanced MRI using ultra-short TE and inversion recovery turbo FLASH. Magn Reson Med 1996; 36:503–508.
4. Uematsu H, Yamada H, Sadato N, et al. Multiple single sections turbo FLASH MR arterial portography in the detection of hepatic neoplasms. Eur J Radiol 1998; 26:257–260.
5. Rosen BR, Belliveau JW, Chien D. Perfusion imaging by nuclear magnetic resonance. Magn Reson Q 1989; 5:263–281.
6. Edelman RR, Mattle HP, Atkinson DJ, et al. Cerebral blood flow: assessment with dynamic contrast-enhanced T2*-weighted MR imaging at 1.5 T. Radiology 1990; 176:211–220.
7. Rempp KA, Brix G, Wenz F, Becker CR, Gückel F, Lorenz WJ. Quantification of regional cerebral blood flow and volume with dynamic susceptibility contrast-enhanced MR imaging. Radiology 1994; 193:637–641.
8. Warach S, Li W, Ronthal M, Edelman RR. Acute cerebral ischemia: evaluation with dynamic contrast-enhanced MR imaging and MR angiography. Radiology 1992; 182:41–47.
9. Belliveau JW, Rosen BR, Kantor HL, et al. Functional cerebral imaging by susceptibility-contrast NMR. Magn Reson Med 1990; 14: 538–546.
10. Maeda M, Itoh S, Kimura H, et al. Vascularity of meningiomas and neuromas: assessment with dynamic susceptibility-contrast MR imaging. AJR Am J Roentgenol 1994; 163:181–186.
11. Bruening R, Kwong KK, Vevea MJ, et al. Echo-planar MR determination of relative cerebral blood volume in human brain tumors: T1 versus T2 weighting. AJNR Am J Neuroradiol 1996; 17:831–840.
12. Bruening R, Wu RH, Yousry TA, et al. Regional relative blood volume MR maps of meningiomas before and after partial embolization. J Comput Assist Tomogr 1998; 22:104–110.
13. Aronen HJ, Gazit IE, Louis DN, et al. Cerebral blood volume maps of gliomas: comparison with tumor grade and histologic findings. Radiology 1994; 191:41–51.
14. Miyati T, Banno T, Mase M, et al. Dual dynamic contrast-enhanced MR imaging. J Magn Reson Imaging 1997; 7:230–235.
15. Wenz F, Rempp K, He T, et al. Effect of radiation on blood volume in low-grade astrocytomas and normal brain tissue: quantification with dynamic susceptibility contrast MR imaging. AJR Am J Roentgenol 1996; 166:187–193.
16. Thompson HK, Starmer F, Whalen RE, McIntosh HD. Indicator transit time considered as a gamma variate. Circ Res 1964; 14:502–515.
17. Schad LR, Brix G, Zuna I, Harle W, Lorenz WJ, Semmler W. Multiexponential proton spin-spin relaxation in MR imaging of human brain tumors. J Comput Assist Tomogr 1989; 13:577–587.
18. Tofts PS, Kermode AG. Measurement of blood-brain barrier permeability and leakage space using dynamic MR imaging. I. Fundamental concepts. Magn Reson Med 1991; 17:357–367.
19. Tofts PS, Berkowitz B, Schnall MD. Quantitative analysis of dynamic Gd-DTPA enhancement in breast tumors using a permeability model. Magn Reson Med 1995; 33:564–568.
20. Tokumaru A, O'uchi T, Eguchi T, et al. Prominent meningeal enhancement adjacent to meningioma on Gd-DTPA-enhanced MR images: histopathologic correlation. Radiology 1990; 175:431–433.
21. Mikhael MA, Ciric IS, Wolff AP. Differentiation of cerebellopontine angle neuromas and meningiomas with MR imaging. J Comput Assist Tomogr 1985; 9:852–856.
22. Just M, Thelen M. Tissue characterization with T1, T2, and proton density values: results in 160 patients with brain tumors. Radiology 1988; 169:779–785.
23. Watabe T, Azuma T. T1 and T2 measurement of meningiomas and neuromas before and after Gd-DTPA. AJNR Am J Neuroradiol 1989; 10:463–470.
24. Long DM. Vascular ultrastructure in human meningiomas and schwannomas. J Neurosurg 1973; 38:409–419.
25. Zieler KL. Theoretical basis of indicator volume. Circ Res 1965; 16:393–407.
26. Wehrli FW. Principles of magnetic resonance. In: Stark DD, Bradley WG, eds. Magnetic resonance imaging. 2nd ed. St Louis, Mo: Mosby–Year Book, 1992; 3–20.